

Basic mechanisms in the laser control of non-Markovian dynamicsR. Puthumpally-Joseph,^{1,2} E. Mangaud,³ V. Chevet,⁴ M. Desouter-Lecomte,^{4,5} D. Sugny,^{1,6} and O. Atabek²¹*Laboratoire Interdisciplinaire Carnot de Bourgogne (ICB), UMR 6303 CNRS-Université Bourgogne Franche Comté, 9 Avenue A. Savary, Boîte Postale 47 870, F-21078 Dijon Cedex, France*²*Institut des Sciences Moléculaires d'Orsay (ISMO) UMR CNRS 8214, Université Paris Saclay, Université Paris Sud, F-91405 Orsay, France*³*Laboratoire Collisions Agrégats Réactivité (IRSAMC), Université Toulouse III Paul Sabatier, UMR 5589, F-31062 Toulouse Cedex 09, France*⁴*Laboratoire Chimie Physique (LCP)-CNRS, Université Paris Saclay, Université Paris Sud, F-91405 Orsay, France*⁵*Département de Chimie, Université de Liège, Sart Tilman, B6, B-4000 Liège, Belgium*⁶*Institute for Advanced Study, Technische Universität München, Lichtenbergstrasse 2 a, D-85748 Garching, Germany*

(Received 19 October 2017; published 27 March 2018)

Referring to a Fano-type model qualitative analogy we develop a comprehensive basic mechanism for the laser control of the non-Markovian bath response and fully implement it in a realistic control scheme, in strongly coupled open quantum systems. Converged hierarchical equations of motion are worked out to numerically solve the master equation of a spin-boson Hamiltonian to reach the reduced electronic density matrix of a heterojunction in the presence of strong terahertz laser pulses. Robust and efficient control is achieved increasing by a factor of 2 the non-Markovianity measured by the time evolution of the volume of accessible states. The consequences of such fields on the central system populations and coherence are examined, putting the emphasis on the relation between the increase of non-Markovianity and the slowing down of decoherence processes.

DOI: [10.1103/PhysRevA.97.033411](https://doi.org/10.1103/PhysRevA.97.033411)**I. INTRODUCTION**

Nonunitary dynamics among quantum states of a subsystem coupled to its environment involving a large number of degrees of freedom, where dissipation and decoherence evolve simultaneously, is the basic concern of the theory of open quantum systems (OQSs) [1–7]. Since no physical system can truly be considered isolated, OQSs are actually very common, not only in physics but also in chemistry and biology, where they have recently attracted considerable attention in applications ranging from quantum technologies in the condensed phase, to electronic and proton transfers in flexible proteins [8]. But even more important is to build quantum control strategies to optimize physical observables [9,10] such as decoherence rates or efficient and fast charge transfers over large molecular structures, with final challenges as crucial as light harvesting in photosynthetic organisms [11–13].

When aiming at controlling OQSs over a wide range of time, energy, or temperature, the environmental bath response to the central system can no longer be neglected. As a consequence, this induces large memory effects with non-Markovian evolution describing dissipation and decoherence that should appropriately be taken into account [3,4]. In other words, any control exerted on the central system would be limited in time and robustness by the unavoidable dissipation towards the bath [9,10,14–20]. The ultimate challenge should be to take advantage of the backflow of information characterizing non-Markovianity—to control the central system's physical observables [21,22]. Said differently, the question of the extent to which appropriately controlling memory effects (i.e., non-Markovianity or entropy, for instance), fighting against decoherence, would affect the robustness of the central system

characteristics, protecting them from dissipation, is of major interest. Three strategies to reach this goal can be proposed:

(i) Acting on the central system alone, through a strong static dc field, produces a Stark shift among the eigenenergies of the two-level system. Enhanced non-Markovianity is expected from off-resonant excitation [23]. The present work is precisely dedicated to the implementation and generalization of such strategies to intense laser field controls. Moreover, we are observing the consequences of increased non-Markovianity on the central system populations and coherence.

(ii) Still acting on the central system alone, but now using an optimal control scheme aiming at some protection against decoherence of its physical characteristics (population revival or robust exchange), we can observe the consequences in terms of the bath non-Markovian response. This analysis which goes beyond the scope of this paper will be published elsewhere [24].

(iii) Using local control in an appropriate way to increase some non-Markovianity witnesses (volume of accessible states, entropy, or free energy), we relate this response with its expected consequences, such as less dissipative central system observables. This future prospect, i.e., taking advantage of non-Markovianity for a robust control of the full system dynamics, would presumably require, for its efficiency, acting on both the central system and its environmental bath in a direct way. This could be reached by referring to some collective modes which guide the flow of information from the central system to the bath in a reversible manner [3].

It is, however, to be noted that even if the control field is assumed to explicitly have a dipole interaction with the central system only, it still has an influence on the bath dynamics

through a memory kernel involved in the master equation driving the central system evolution [25–27].

Control referring to external fields has also been the purpose of some recent works in the literature. Among others, we can mention Ref. [22], where the authors show that a periodical modulation of the driving field can enhance the non-Markovian behavior of an open quantum system. In Ref. [28], the degree of non-Markovianity for a driven system is investigated for a finite-size environment. The interplay between driving and non-Markovianity is also studied in Ref. [29] with a quantum thermodynamic perspective. The validity of the fixed-dissipator assumption for driven non-Markovian open quantum systems is discussed in Ref. [30]. The role of initial correlations between the system and the bath is shown in the speedup of control processes in Ref. [31].

The paper is organized as follows. In Sec. II, a spin-boson Hamiltonian [1,32] is worked out, referring to realistic parameters taken from a model heterojunction between fullerene and oligothiophene molecules [33–35]. The dynamics of the central system density matrix described by a non-Markovian master equation is solved using the so-called hierarchical equations of motion (HEOM) up to convergence [36–38]. Stark shift as a basic mechanism for non-Markovianity is introduced through a qualitative Fano-type analogy and fully implemented in a realistic laser control scheme. The time evolution of the volume of accessible states illustrated on an appropriate Bloch sphere is taken as a measure of non-Markovianity [39]. We emphasize that several other recent publications [40–42], although dealing with time-dependent fields within the HEOM formalism, have actually not explicitly addressed non-Markovianity enhancement, as is done in the present work. Section III is dedicated to the presentation of the results. The external control fields are chosen both as realistic ultrashort-duration dc flashes, or terahertz single optical cycle pulses with intensities less than 5×10^{12} W/cm². The major result is a spectacular enhancement of non-Markovianity that could be achieved through a tunable Stark shift, which thus turns out to be a basic control mechanism for such OQSs. Finally, the response to such a control of the central system's physical observables (populations and coherence) is investigated. Additionally, Supplemental Material is provided [43] to illustrate a typical trajectory of a Bloch vector and the time evolution of the volume in field-free and field-controlled cases.

II. MODEL AND THEORY

A. The spin-boson Hamiltonian

Having in mind a donor-acceptor type of charge-transfer process, we consider a fullerene-oligothiophene heterojunction modeled by a molecular dimer within a two-level approximation making up the central system S [33–35]. More precisely, a spinlike Hamiltonian H_S describes two electronic states $|1\rangle$ and $|2\rangle$ of a diabatic representation, radiatively coupled through a dipole interaction. The 2×2 matrix representation of H_S (in atomic units [a.u.], where $\hbar = 1$) is given by

$$H_S(t) = \delta\sigma_z + W\sigma_x - \boldsymbol{\mu}E(t), \quad (1)$$

where σ_x and σ_z are the corresponding Pauli matrices, 2δ measures the diabatic energy gap between $|1\rangle$ and $|2\rangle$, and

W is the interstate potential electronic coupling. Their actual values are those corresponding to the heterojunction with an interfragment distance fixed at $R = 2.5 \text{ \AA}$, leading to $2\delta = 0.517 \text{ eV}$ and $W = 0.2 \text{ eV}$. This amounts to an eigenenergy gap of $\omega_0 = 0.654 \text{ eV}$ (that is, 0.024 a.u.) in the adiabatic basis obtained by diagonalizing the field-free Hamiltonian, with a corresponding Rabi period of 6.3 fs . As for the dipole matrix $\boldsymbol{\mu}$, it is the only quantity entering the model that is not yet calculated from quantum chemistry codes. For our donor-acceptor system, we model it, in the diabatic basis, as a diagonal matrix

$$\boldsymbol{\mu} = \mu_0\sigma_z = \mu_0 \begin{bmatrix} 1 & 0 \\ 0 & -1 \end{bmatrix}, \quad (2)$$

assuming a typical value $\mu_0 = 1 \text{ a.u.}$ Finally, the time-dependent electric field amplitude is denoted $E(t)$ and the resulting time dependence of $H_S(t)$ occurs only through the radiative coupling in the length gauge, $-\boldsymbol{\mu}E(t)$, with the additional assumption that the dipole vector is aligned with the linearly polarized electric field [44]. It is worth noting that, even if the experimental feasibility of such an alignment is questionable, the ultrashort pulse durations we are referring to are such that the molecular fragment rotational dynamics can safely be assumed as frozen.

All nuclear degrees of freedom involved in the vibronic description of the heterojunction are associated with a bosonic bath. More precisely, this bath collects all normal modes of the two oligothiophene-fullerene fragments. The bosonic time-independent part of the Hamiltonian is written in terms of (mass-weighted) nuclear coordinates q_k and their associated momenta p_k , k labeling a given harmonic oscillator associated to a normal mode:

$$H_{\text{boson}} = \mathbf{I} \frac{1}{2} \sum_{k=1}^N [p_k^2 + \omega_k^2(q_k \pm d_k/2)^2], \quad (3)$$

where d_k are the spatial shifts between equilibrium geometries in the two electronic states. Actually, d_k 's are responsible for the central system-bath couplings (vibronic couplings) as it is clearly shown when displaying H_{boson} in three terms:

$$H_{\text{boson}} = H_B + H_{\text{SB}} + H_{\text{ren}} \quad (4)$$

with

$$H_B = \mathbf{I} \frac{1}{2} \sum_{k=1}^N [p_k^2 + \omega_k^2 q_k^2], \quad (5)$$

$$H_{\text{SB}} = B\sigma_z, \quad B = \sum_{k=1}^N c_k q_k, \quad (6)$$

and

$$H_{\text{ren}} = \mathbf{I} \sum_{k=1}^N (c_k/\sqrt{2}\omega_k)^2, \quad (7)$$

where H_B is the bath Hamiltonian, H_{SB} is the system-bath coupling, B is a collective bath coordinate with vibronic coupling coefficients $c_k = \omega_k^2 d_k/2$ involving d_k , H_{ren} is an energy renormalization, and \mathbf{I} is the unitary matrix in the system space. In the following, $N = 264$ normal modes are

TABLE I. Parameters for spectral density $\mathcal{J}(\omega)$.

| p_k (a.u.) | Ω_k (a.u.) | Γ_k (a.u.) |
|------------------------|-----------------------|--------------------|
| 3.72×10^{-10} | 6.99×10^{-3} | 5.86×10^4 |
| 1.90×10^{-11} | 3.05×10^{-3} | 5.50×10^4 |
| 7.80×10^{-12} | 4.00×10^{-3} | 4.70×10^4 |
| 5.80×10^{-12} | 1.94×10^{-3} | 6.83×10^4 |
| 8.00×10^{-12} | 5.20×10^{-3} | 7.00×10^4 |

retained and their frequencies ω_k are assumed to be the same in both electronic states $|1\rangle$ and $|2\rangle$. It is shown that an alternate way to fully characterize the spin-boson coupling is through a spectral density written as a frequency comb [2]:

$$\mathcal{J}(\omega) = \frac{\pi}{2} \sum_k \frac{c_k^2}{\omega_k} \delta(\omega - \omega_k). \quad (8)$$

In our heterojunction case, the spectral density is given as a continuous functional form [25,45]

$$\mathcal{J}(\omega) = \sum_{k=1}^M \frac{\omega p_k}{[(\omega - \Omega_k)^2 + \Gamma_k^2][(\omega + \Omega_k)^2 + \Gamma_k^2]}, \quad (9)$$

with all fit parameters (up to $M = 5$) provided in Table I.

In summary, apart from the dipole matrix, all parameters entering the spin (energy gap and residual diabatic interstate coupling) and bosonic (spectral density) parts are those of the heterojunction characterized by its interfragment geometry.

B. The non-Markovian master equation

The key observable in OQS dissipative dynamics is the reduced density matrix ρ which is given as the partial trace, over bath degrees of freedom, of the full density matrix Ξ :

$$\rho(t) = \text{Tr}_B[\Xi(t)]. \quad (10)$$

Projection techniques used within the Nakajima-Zwanzig [2] formalism lead to a non-Markovian master equation which could be recast as

$$\partial_t \rho(t) = \mathcal{L}_{\text{eff}}(t) \rho(t) + \int_0^t dt' K(t, t') \rho(t'), \quad (11)$$

where the effective Liouvillian reads

$$\mathcal{L}_{\text{eff}}(t) \rho(t) = -i[(H_s(t) + H_{\text{ren}}), \rho(t)] \quad (12)$$

and $K(t, t')$ is the already-mentioned memory kernel. The solution of Eq. (11) requires an initial condition for which a separability between the central system and the bath is assumed at $t = 0$:

$$\Xi(0) = \rho(0) \rho_{\text{eq}}, \quad (13)$$

ρ_{eq} being the bath density matrix at thermal equilibrium. For complex systems the most challenging part is the numerical evaluation of the memory kernel. In this work we are using a well-known strategy based on HEOM [36–38]. One of the requirements of this method, referring to path-integral techniques, is an exponential expansion of the correlation function of the collective bath mode B defined in Eq. (6). Actually, the fluctuation-dissipation theorem relates the correlation function

\mathcal{C} to the bath spectral density \mathcal{J} [2]:

$$\mathcal{C}(t, t_0) = \frac{1}{\pi} \int_{-\infty}^{+\infty} \frac{e^{-i\omega(t-t_0)}}{1 - e^{-\beta\omega}} \mathcal{J}(\omega) d\omega, \quad (14)$$

where the bath temperature T enters in $\beta = 1/k_B T$, k_B being the Boltzmann factor. With the two-pole Lorentzian form of \mathcal{J} , referring to Cauchy's residue theorem when evaluating the integral in Eq. (14), the correlation function and its complex conjugate are finally written as [46]

$$\mathcal{C}(t) = \sum_{k=1}^{n_{\text{cor}}} \alpha_k e^{i\zeta_k t} \quad (15)$$

and

$$\mathcal{C}^*(t) = \sum_{k=1}^{n_{\text{cor}}} \tilde{\alpha}_k e^{i\zeta_k t}. \quad (16)$$

The solution of Eq. (11) turns out to be the first element of a chain of auxiliary density matrices $\rho_{\mathbf{n}}(t)$ obeying a system of coupled equations written as

$$\begin{aligned} \dot{\rho}_{\mathbf{n}}(t) = & -i[H_S(t), \rho_{\mathbf{n}}(t)] + i \sum_{k=1}^{n_{\text{cor}}} n_k \zeta_k \rho_{\mathbf{n}}(t) \\ & - i \left[\sigma_z, \sum_{k=1}^{n_{\text{cor}}} \rho_{\mathbf{n}_k^+}(t) \right] - i \sum_{k=1}^{n_{\text{cor}}} n_k (\alpha_k \sigma_z \rho_{\mathbf{n}_k^-} - \tilde{\alpha}_k \rho_{\mathbf{n}_k^-} \sigma_z), \end{aligned} \quad (17)$$

where $\mathbf{n}_k = (n_1, \dots, n_{n_{\text{cor}}})$ is a vector giving the occupation numbers in the n_{cor} dissipative modes involved in the decomposition of $\mathcal{C}(t)$ and $\mathbf{n}_k^{\pm} = (n_1, \dots, n_k \pm 1, \dots, n_{n_{\text{cor}}})$. The level L of an auxiliary matrix in the hierarchy corresponds to the sum $L = \sum_{k=1}^{n_{\text{cor}}} n_k$. The mathematical structure is such that each density matrix of level L is coupled to matrices of level $L \pm 1$, and $L = 0$ leads to $\rho(t) = \rho_0$ with all occupation numbers zero. Equation (17) is solved at a given level of hierarchy L , corresponding to a given approximation. It is worth noting that the first moment of the collective mode B , given as $X^1 = \text{Tr}_B[B \Xi(t)]$, may help for a better understanding of the correlated system-bath dynamics. The HEOM formalism provides a direct evaluation of X^1 in terms of the first-level auxiliary matrices (with \mathbf{n} such that $\sum_{k=1}^{n_{\text{cor}}} n_k = 1$) [35]:

$$X^1(t) = - \sum_{\mathbf{n}} \rho_{\mathbf{n}}(t). \quad (18)$$

In particular, the importance of memory effects in Eq. (11) can directly be probed through this first moment upon recasting it in the master equation, leading finally to [47]

$$\dot{\rho}(t) = -i[H_S(t), \rho(t)] + i[\sigma_z, X^1(t)]. \quad (19)$$

C. Basic mechanism for control

The spectral density $\mathcal{J}(\omega)$ is displayed in Fig. 1(a) and its corresponding correlation function $\mathcal{C}(t)$ at room temperature in Fig. 1(b). In the absence of an external field, the two adiabatic eigenlevels of the central system are only indirectly coupled through their environmental bath. $\mathcal{J}(\omega)$ can be viewed as a frequency representation of an energy-dependent discrete-continuum coupling scheme appropriately averaged over the

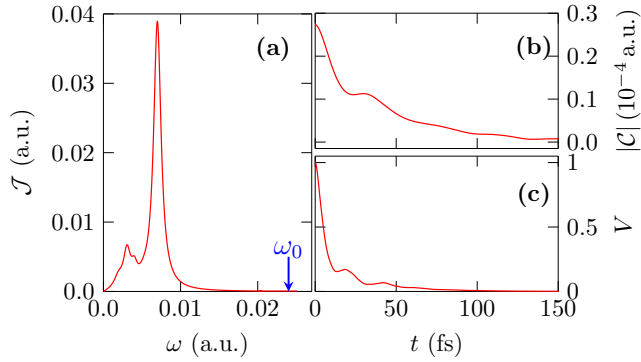


FIG. 1. (a) The spectral density $\mathcal{J}(\omega)$, (b) the square modulus of the corresponding correlation function $|\mathcal{C}(t)|$ in a.u. at $T = 300$ K, and (c) the volume of accessible states $V(t)$ (dimensionless, calibrated to 1 at $t = 0$). The gap between the two levels, $\omega_0 = 0.024$ a.u., is indicated by the blue vertical arrow in (a).

density of levels of the discretized quasicontinuum. In that respect, the spin-boson model could be put in analogy with a standard Fano resonance representation of two discrete states (central system) facing and interacting [48,49] [through $\mathcal{J}(\omega)$] with a discretized quasicontinuum (set of bath harmonic oscillators). A highly structured $\mathcal{J}(\omega)$, such as the one in Fig. 1 with two well-peaked Lorentzians, is expected to lead to important memory effects. Such narrow peaks could be attributed to some long-lived Feshbach resonances that are locally modifying the density of states. They are supporting bath collective modes and due to their long enough lifetimes could temporarily trap the system-bath dynamics, or efficiently mediate it, ultimately leading to enhanced non-Markovianity. Even more important for the control purpose is the central system transition frequency ω_0 which can be progressively tuned through the variation of the external field amplitude $E(t)$. As has previously been discussed, two extreme situations can be considered: the on-resonant case, when ω_0 matches one of the two maxima of $\mathcal{J}(\omega)$, and the off-resonant case otherwise [50]. The latter is expected to produce the most important memory effects. However, it should be emphasized that the different cases we are dealing with in this work turn out to be basically off-resonant situations. Consequently, the Fano-inspired model to rationalize them has to be accordingly refined. Actually for the off-resonant case the central system is only weakly coupled to the bath (low values of the spectral density corresponding to ω_0). The backflow of information from the bath to the central system is organized along two strategies in competition: either (i) on the energy shell, i.e., at the same frequency as ω_0 but with a low system-bath coupling, or (ii) off the energy shell, i.e., at frequencies corresponding to local maxima of the spectral density with large system-bath couplings. The latter strategy requires absorption of additional photons or excitation of phonons and proceeds from longer times, leading to non-Markovianity. The availability of adequate phonon frequencies of bath normal modes for the internal transitions to occur has also to be taken into account. The specific peaked structure of the spectral density offers thus a rather large control flexibility by tuning ω_0 . As has been previously suggested, this is expected to be achieved through an external field producing a fully controlled Stark shift among

the levels of the central system via their transition dipole [23]. The strategy followed hereafter is precisely based on this adaptable Stark shift, taken as a basic mechanism. However, the control field indirectly affects the bath dynamics and does not completely disentangle the action over the central system from the bath.

D. Non-Markovian evolution of the volume

Several witnesses of non-Markovianity have recently been discussed in the literature [3,50,51], among which are the volume of accessible states [52], the associated decoherence rate of a time-dependent Lindblad-type evolution [53,54], and the von Neumann entropy [55]. More precisely, the time evolution of the central system density matrix can be written through a quantum dynamical map $F(t)$ by expanding the density matrix in a (2×2) basis set of Hermitian operators and an initial condition [52]

$$\tilde{\rho}(t) = F(t)\tilde{\rho}(0), \quad \text{for } t \geq 0. \quad (20)$$

Assuming nonsingularity of $F(t)$ at time t , differentiating Eq. (20), one gets a time-local matrix equation:

$$\dot{\tilde{\rho}}(t) = \mathcal{L}(t)\tilde{\rho}(t) = \dot{F}F^{-1}\tilde{\rho}(t). \quad (21)$$

The non-Markovian character is associated with the relaxation rate of the generator \mathcal{L} . The volume of accessible states, $V(t)$, is obtained by mapping the density matrix to its corresponding Bloch sphere using the complete orthogonal basis set of Pauli matrices together with the identity. The time evolution of the volume of this Bloch ball, $V(t)$, is then given by the determinant of $F(t)$, a quantity independent of any initial condition:

$$V(t) = \det[F(t)]. \quad (22)$$

It can also be shown that the total decoherence rate $\Gamma(t)$ of \mathcal{L} is related to the volume through [53]

$$V(t) = V(0) \exp \left[-d \int_0^t \Gamma(t') dt' \right], \quad (23)$$

where d is the dimension of the space (here $d = 2$). Finally, the dynamics is said to be non-Markovian if

$$\frac{dV(t)}{dt} \geq 0 \quad (24)$$

or, equivalently, if $\Gamma(t) < 0$, as opposite to a situation where the total decay rate is always positive. A backflow of information from the bath to the central system can be observed for values of $\Gamma(t)$ temporarily negative. Then the time evolution of the volume departs from pure exponential decay and may even show some bumps which turn out to be clear signatures of non-Markovianity [39].

III. RESULTS AND DISCUSSION

The numerical results are presented in three sections discussing the following aspects: (i) determination of generic field parameters and convergence of the associated dynamical evolution calculations with respect to successive orders of HEOM, (ii) evolution of the volume and of the total decoherence rate as resulting from specific control fields, and (iii) consequences of the control of non-Markovianity on the time evolution of

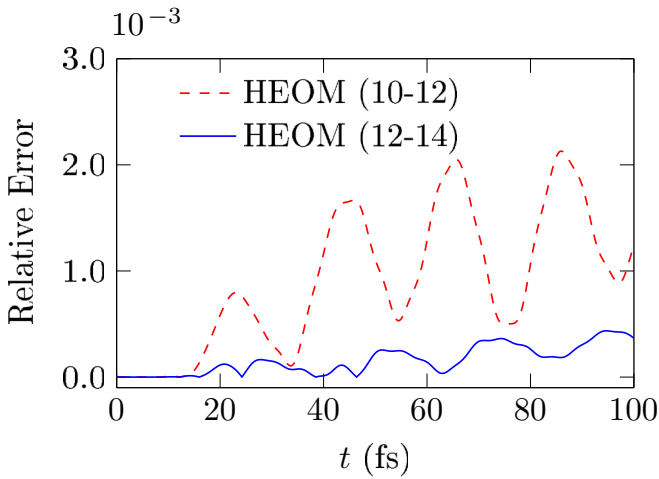


FIG. 2. Relative error in $V(t)$ calculated for successive $2L$ orders of HEOM. Dashed red curve is the error in $V(t)$ between orders 10 and 12, while the solid blue curve is the same for orders 12 and 14.

physical observables such as populations of the initial state, coherence, and bath collective modes.

A. HEOM convergence

Figure 1 illustrates, together with the spectral density and the corresponding evolution of the correlation function, the time-dependent volume of accessible states, in field-free conditions. A typical time scale for the overall decay process could be estimated as about 60 fs, after which the correlation function has decayed to almost one-third of its initial value and the volume to almost zero. Our first purpose is to check the numerical convergence when solving Eq. (17) as a function of increasing level L of hierarchy which corresponds to perturbation order $2L$. This is done, in a field-free situation, by evaluating the relative error affecting the volume, that is, $[V(2L+2) - V(2L)]/V(2L)$, when increasing $2L$. The results are displayed in Fig. 2 as a function of time up to 100 fs. For the perturbation order $2L = 10$ the relative error remains less than 2×10^{-3} for the overall dynamics with some oscillations occurring at about 25 and 45 fs, roughly corresponding to times leading to a plateau behavior of the correlation function. When increasing the level of hierarchy, at perturbation order $2L = 12$, the relative error is clearly attenuated and no longer exceeds 0.5×10^{-3} , which seems to be acceptable for an overall characterization of the volume. To avoid highly time-consuming calculations we fix $2L = 12$ for the convergence criterion. The required perturbation order in HEOM basically depends on the importance of the central system-bath coupling, given by the spectral density. The inclusion of a control field, even a strong one, within the central system would only indirectly affect these couplings. The relevance of the convergence criterion set for the field-free case has successfully been checked for the field-driven dynamics.

Finally, it is also interesting to note that the volume is not decaying monotonously but shows two bumps of modest amplitude at about 25 and 40 fs. These are signatures of non-Markovianity presumably due to an off-resonant configuration

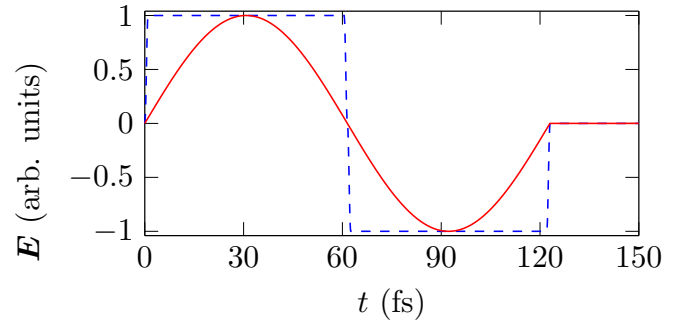


FIG. 3. Typical profiles of the electric fields used in the calculations, in arbitrary units. The dashed blue curve indicates the dc flash and the solid red curve indicates the ac sine pulse.

and specific spectral density of our model heterojunction. Actually, the transition frequency ω_0 is larger than the frequency corresponding to the maximum amplitude of $\mathcal{J}(\omega)$, $\omega_{\max} = 0.007$ a.u. Our control goal is to enhance non-Markovian signatures (amplitude of the bumps) by positively or negatively Stark shifting the energy levels of the central system, tuning the already off-resonant ω_0 , through the application of control fields.

B. Control fields

Two types of generic fields for achieving control based on the Stark shift mechanism are displayed in Fig. 3: a static dc field with positive or negative amplitudes, and a corresponding single optical cycle laser pulse with the same period satisfying the Maxwell equations requirement of a zero time-integrated area [56]. The half period is taken as 60 fs, basically in relation with typical decaying behaviors of the correlation function and the volume, which display a monotonic decrease at times later than 60 fs with almost negligible values. The positive or negative amplitudes of the dc field are used to produce sudden negative or positive Stark shifts. As for the sine function describing the laser pulse, it is expected to provide an adiabatically switched time-dependent excitation producing progressively the Stark shift which is sought.

Inspired by and analogous with the Fano model, we provide a numerical proof of the Stark shift mechanism on the non-Markovian control of the bath response by calculating the volume of accessible states for a collection of increasing dc field amplitudes ranging from $E = 1.43 \times 10^{-5}$ to $E = 9.97 \times 10^{-5}$ a.u. (leading to intensities ranging from 5×10^{11} up to 3.5×10^{12} W/cm²). Such fields produce transition-frequency gaps in the two-level system ranging from 0.015 to 0.042 a.u.. When comparing with the field-free transition frequency $\omega_0 = 0.024$ a.u., both lower and higher shifts are observed (i.e., positive or negative contributions of the control fields). But, most importantly, all situations which are depicted are nonresonant with respect to $\omega_{\max} = 0.007$ a.u. It has to be emphasized that the Fano-type model interpretation can favor either positive or negative Stark shifts mediating off-the-energy-shell processes that are in competition in such nonresonant cases, putting the system transition frequency farther from or closer to the maximum spectral density frequency.

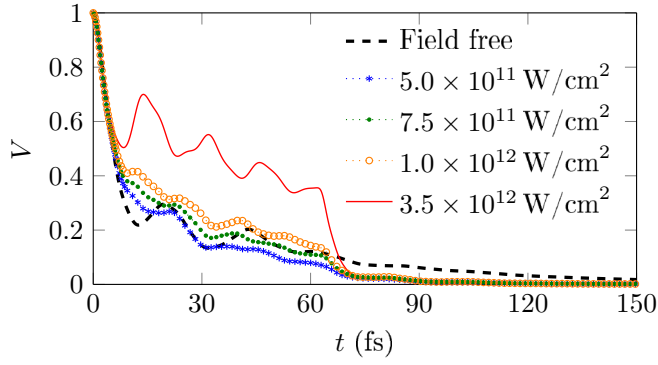


FIG. 4. Time evolution of the volume V of accessible states in the Bloch sphere for different intensities of ultrashort dc flash. V calibrated to 1 at $t = 0$ is dimensionless.

The results of the corresponding time evolution of the volume are gathered in Fig. 4. Several points are in order:

(i) For times $t \leq 60$ fs a noticeable enhancement of non-Markovianity is observed for intensities of the order of 1×10^{12} W/cm², both with respect to the slowing down of the overall decaying behavior and especially for the increasing amplitude of the bumps.

(ii) Such signatures are very much enhanced with stronger fields resulting in bumps with spectacular amplitudes reaching about 20% of the initial value, and an overall decay which does not exceed 40% at time $t = 60$ fs, as compared with a value of about 10% for the field-free case. The bump periodicity (about 15 fs) is less than that of the field-free case (about 20 fs). This could be related to two effects, namely, the variation of the Rabi transition period of the central system and the indirect action of the control field on the bath.

(iii) For times exceeding 60 fs, when the Stark shift becomes negative, still in conformity with the Fano-model analogy, all previous dynamical behaviors are reversed, with a rather sudden decay much faster than the field-free case.

In summary, an efficient control of non-Markovianity referring to strong dc fields seems thus achievable. However, the experimental feasibility of such intense electric fields is questionable, despite their ultrashort duration (60 fs), which makes them dc flashes rather than static dc fields. This is why we now address midinfrared or terahertz laser fields with the same periodicity (8 THz, 36 μ m wavelength) and comparable intensities, as illustrated in Fig. 3 with the expectation that they will also provide efficient enough control tools.

C. Laser control of non-Markovianity

With typical control parameters already fixed for ultrashort dc flashes, we now proceed to more realistic laser control by referring to single optical cycle terahertz laser pulses of 12 μ m wavelength and intensity of 3.5×10^{12} W/cm². Two phases are considered, leading to electric field amplitudes starting either with positive or negative values. Figure 5 gathers the results for HEOM converged time evolution of the volume $V(t)$ [Eq. (22)] and the total decoherence rate $\Gamma(t)$ [Eq. (23)]. We again observe the markedly different behaviors induced by positive or negative amplitudes rationalized by the off-resonant Fano-model analogy. In the present case, positive

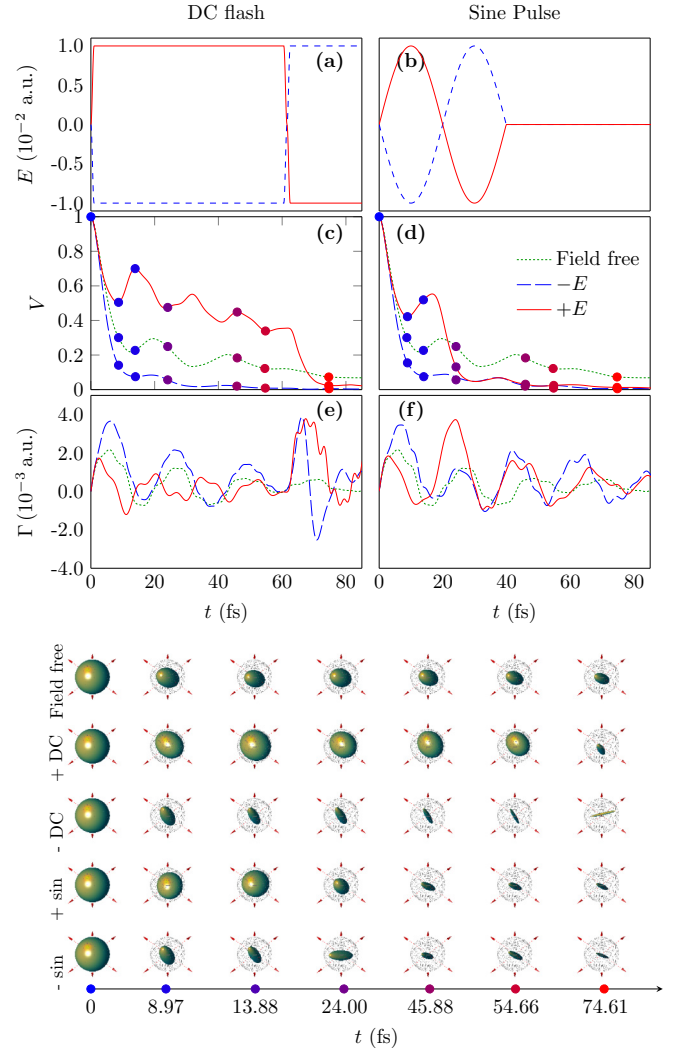


FIG. 5. (a), (b) Time evolution of the electric field amplitudes for a peak intensity of 3.5×10^{12} W/cm². (c), (d) Time evolution of the volume of accessible states (V calibrated to 1 at $t = 0$ is dimensionless). (e), (f) Time evolution of the sum of canonical rates in atomic units. The dotted green curve is for the field free case. The solid red and blue curves respectively indicate the positive and negative initial values of the field amplitude. The bottom panel displays three-dimensional illustrations of the Bloch ball evolution (volume of accessible states) at specific times corresponding to the dots of (c) and (d).

amplitudes (inducing negative Stark shifts) produce reduced transition frequencies increasing non-Markovianity, whereas negative ones (inducing positive Stark shifts) lead to very fast and more monotonous memory decay processes. But, more importantly, terahertz laser pulses inducing a dynamical Stark shift of comparable amplitude with the ultrashort dc flash, at least close to its maximum time, are actually shown to provide very efficient non-Markovianity control. This is clearly proved by the spectacular enhancement of the first bump in the volume at about 20 fs. As compared with the field-free case the volume almost exhibits a twofold enhancement which could be considered a very promising control achievement, solely and simply based on a comprehensive mechanism.

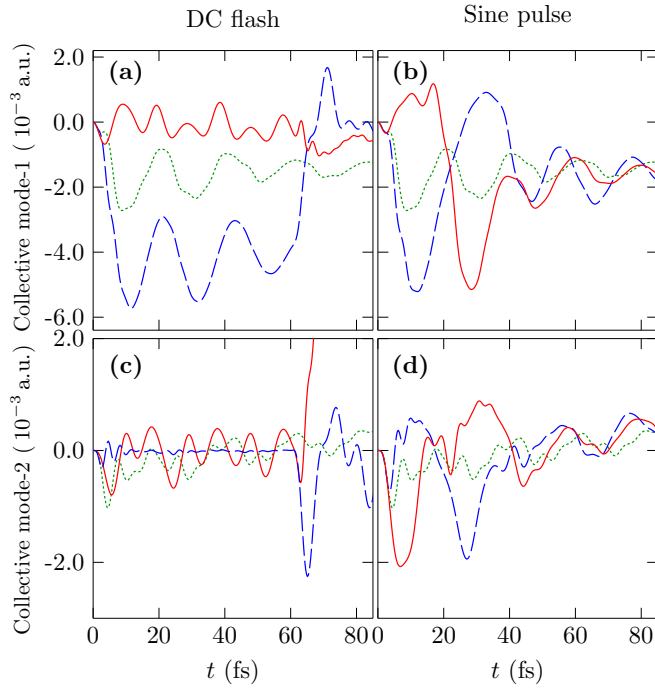


FIG. 6. Time evolution of first moments of the collective mode (in atomic units) in each electronic state for an applied field of intensity $3.5 \times 10^{12} \text{ W/cm}^2$. The dotted green curve indicates the field-free case, the solid red curve indicates the positive values and the dashed blue curve indicates the negative values of the field amplitude.

It is worth noting that such efficiency goes much beyond our expectations from the simple consideration of the basic mechanism as described in Ref. [23] (see Figs. 3 and 4), displaying rather modest non-Markovian behaviors. Moreover, robustness is also an important issue, proven by the control scheme which remains efficient when going from a static field to a few-cycle terahertz pulse. In the lower panel of Fig. 5, it is interesting to notice that the time-dependent behavior of the total decoherence rate $\Gamma(t)$ is quite close for the two dc or ac fields during the increasing amplitude period of the sine pulse, with temporary negative values around 15 fs responsible for the most important bump in the volume. Clearly visible differences appear, however, for the decreasing amplitude part of the sine pulse.

Figure 5 also displays the time evolution of the Bloch-sphere representation of the volume of accessible states, with the following mapping of the density matrix ρ on the position vector $\vec{r}(x, y, z)$:

$$x = 2\text{Re}(\rho_{12}), \quad y = 2\text{Im}(\rho_{12}), \quad z = \rho_{22} - \rho_{11}. \quad (25)$$

These are given at some specific times and help show the different axes along which the volume decreases or temporarily increases, building up the bumps we are referring to as signatures of non-Markovianity. In particular, the Bloch vector evolves through trajectories with much better norm conservation (i.e., longer lasting coherence) when controlled by the external field. Such trajectories and a complete dynamics of the ellipsoidal volume evolving inside the Bloch sphere are illustrated in the Supplemental Material in terms of animated figures (see Figs. S2 and S3 [43]).

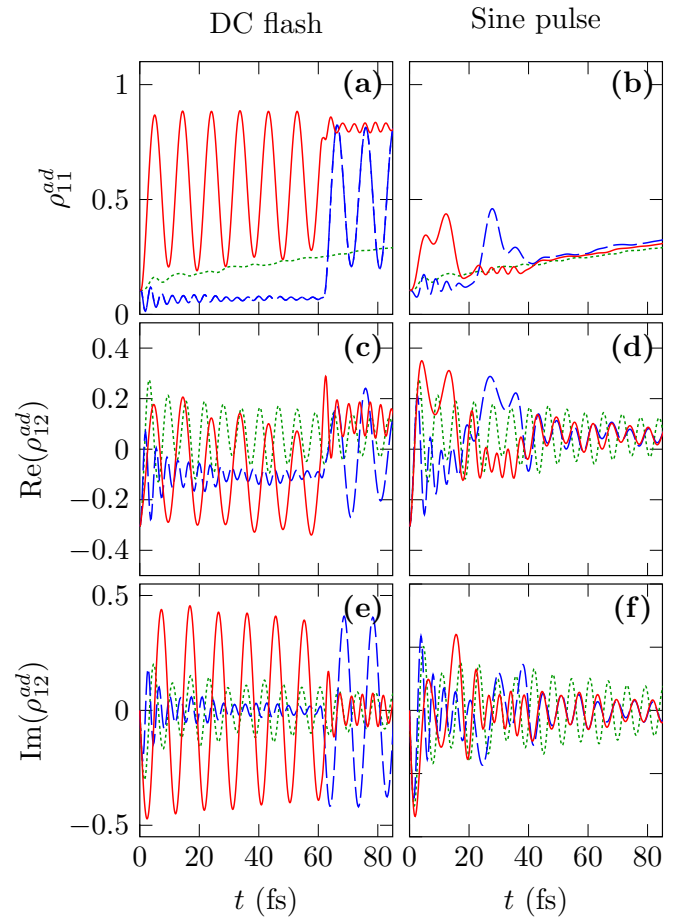


FIG. 7. (a), (b) Adiabatic ground-state population, (c), (d) $\text{Re}(\rho_{12}^{\text{ad}})$, and (e), (f) $\text{Im}(\rho_{12}^{\text{ad}})$ for the heterojunction excited with dc (left column) or ac (right column) fields. The dotted green curve is the field-free case, the solid red curve indicates the positive and the dashed blue curve the negative values of the field amplitude. All parameters are the same as in Fig. 6.

In addition, we also try to get a better understanding of the control field dependence of the first moment of the collective mode in each electronic state given by the diagonal elements of the $X_1(t)$ matrix [Eq. (18)], emphasized as signatures of the field-induced correlated system-bath dynamics. Figure 6 displays the results for the collective mode in each state (1 and 2) as a function of time using the ultrashort dc flashes and the laser sine pulses of the upper panel of Fig. 5, together with their field-free behaviors. Expectation values of the collective mode in states 1 and 2 are enhanced by factors exceeding 2 close to the laser pulse maximum ($t = 10$ fs) with respectively negative (for mode 1) or positive (for mode 2) field strengths. Ultrashort dc flashes produce similar effects on their full duration (60 fs). This shows, in particular, how the strong laser interaction can modify the central system-bath couplings, efficiently building some collective modes in the bath.

D. Consequence of the control on the system characteristic observables

Referring to the Stark shift in the central system transition frequency as a basic mechanism and controlling it through the

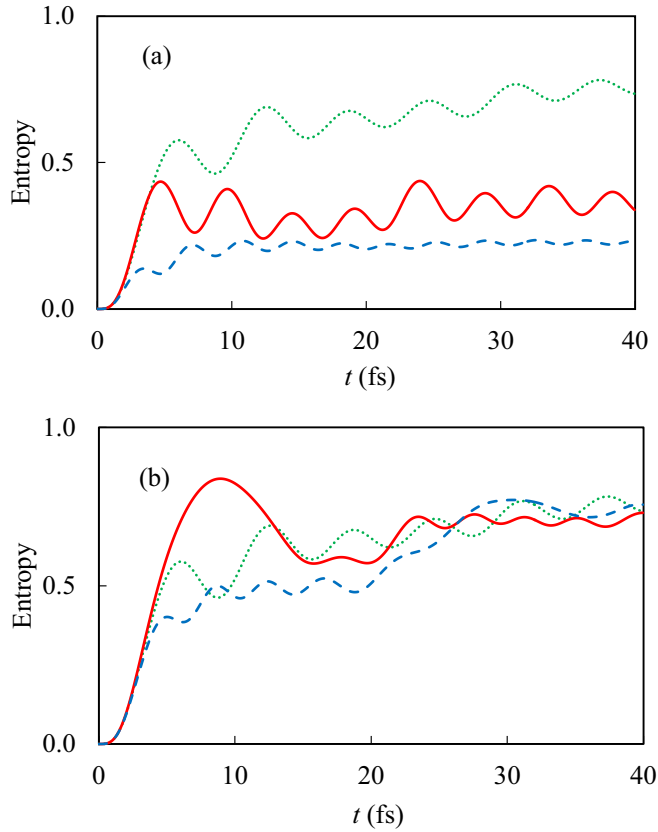


FIG. 8. Entropy of the system: (a) 40-fs ultrashort-duration dc flash and (b) sine pulse of 40 fs period. The dotted green curve indicates the field-free case, the solid red curve indicates the positive and the dashed blue curve indicates the negative values of the field amplitude.

peak intensity of a terahertz laser pulse, we have proceeded to an efficient control of the non-Markovian response of the bath. We wish now to analyze the consequences of such a control on the system's initial-state-dependent physical observables. The initial population in the diabatic representation is ($\rho_{11} = 1$, $\rho_{22} = 0$). The time evolution of the population in the ground eigenstate (adiabatic state) together with the off-diagonal element of the density matrix in this representation, ρ_{12}^{ad} , as a signature of coherence, are displayed in Fig. 7. Positive dc fields rapidly increase ρ_{11}^{ad} and induce typical population oscillations around 1/2. But more interestingly, the amplitude of oscillations in the coherence terms ρ_{12}^{ad} (both real and imaginary parts) are much increased. Similar observations are valid for laser sine pulses, at least for times up to 20 fs (i.e., half-cycle period), even though being much more moderate. Such slowing down of decoherence can be connected with the bumps of the volume evolution and its ellipsoidal shape along the (x, y) axis of Fig. 5.

A last observable is the time evolution of the von Neumann entropy of the central system given by [55]

$$S(t) = -\text{Tr}[\rho(t) \log_2 \rho(t)], \quad (26)$$

which is displayed in Fig. 8. For ultrashort dc flashes (both negative and positive amplitudes), as expected, the entropy is less than the one obtained without the control field all along

the dynamics. The differences, temporarily more than a factor of 2, could be qualified as spectacular. For sine pulses shaped following the dc ones (of period 40 fs as in Fig. 5) an entropy decrease, although much more moderate, is still temporarily observed, for times around $t = 17-23$ fs. It should be noted that these times precisely correspond to bump occurrence in the evolution of the volume of accessible states [Fig. 5(d)] as a signature of non-Markovianity. Later on, apart from low-amplitude oscillations, the evolution of the entropy is no longer affected by the control field. More unexpected is the short time evolution ($t \leq 10$ fs) of the field-controlled entropy showing an important increase and leading to values even higher than the ones of the field-free case. To rationalize such a behavior two points could be emphasized: (i) This short time dynamics is to be related with a fast decay of the volume, where the control field is not efficiently acting on the coherence (as is shown in the Supplemental Material [43]), and (ii) more important is the fast decay of entropy between $t = 10$ fs and $t = 17$ fs (the negative slope of the red curve in Fig. 8), which turns out to be the observable that actually has to be considered as a consequence of non-Markovianity increase.

IV. CONCLUSION

In summary, we are aiming at developing theoretical tools for the laser control of OQSs described by a spin-boson Hamiltonian and solving the Nakajima-Zwanzig master equation referring to a numerical method, involving HEOM at a converged level of the hierarchy. Two steps are followed for this goal: (i) address as a measure of non-Markovianity the nonmonotonous decay of the volume of accessible states and, in particular, the occurrence and amplitude of bumps in its time evolution (i.e., negative total decay rates at particular times) [39] and (ii) identify, in a comprehensive way, a basic laser-induced mechanism to enhance the non-Markovian bath response. Such a response being generically obtained through an appropriate laser pulse, we proceed to the time evolution of the system physical observables and in particular their coherence characteristics. This is done by keeping in mind the following question: How much does enhancing non-Markovianity slow down the decoherence in the density matrix decay, or increase the dynamical entropy?

The illustrative system is the well-documented heterojunction between fullerene and oligothiophene molecules at a fixed interfragment distance. All parameters entering the model, with the exception of the transition dipole taken in a reasonable typical range of magnitude, are the ones provided by previous works. The basic mechanism we are looking for is inferred from a Fano-type model analogy of two discrete levels facing a quasicontinuum with a structured density of levels. This qualitatively gives rise to some comprehensive view of the non-Markovianity increase, at least when the interstate transition frequency is off resonant with respect to the spectral density function peak frequency. A static dc field of appropriate intensity can obviously produce the Stark shift which is sought [23]. This being taken as a possible basic control mechanism, we implement it in a control strategy by adequately shaping a few-cycle terahertz laser pulse. As a consequence, positive or negative time-adapted dynamical Stark shifts are produced, leading to non-Markovianity enhancement. This ultimately

proves the expected efficiency of the basic mechanism we referred to in Ref. [23].

As the most remarkable result of this paper, in a robust and experimentally achievable way, we are increasing by more than a factor of 2 the amplitude of the bumps during the short time evolution of the volume of accessible states, thus considerably enhancing non-Markovianity. The analysis of the consequences on the two-level subsystem reduced density matrix and entropy or bath collective modes shows, although at a rather modest level, a slowing down of decoherence signatures which are promising for future attempts concerned with more sophisticated optimal control tools [9,24]. Actually this is the aim of our future project, that is, referring to control theory for shaping a laser pulse so as to optimally slow down the decoherence dynamics of the central system populations

(protection or rebirth of the initial state, or efficient interstate switching) and/or the increase of its dynamical entropy, to observe the consequences on non-Markovianity signatures, and to show how the two control issues are closely related. We are actively pursuing our research in this direction.

ACKNOWLEDGMENTS

We acknowledge support from the ANR-DFG, under Grant No. ANR-15-CE30-0023-01. This work has been performed with the support of Technische Universität München Institute for Advanced Study, funded by the German Excellence Initiative and the European Union Seventh Framework Program under Grant No. 291763 and within the frame of the French GRD 3575 THEMES.

-
- [1] U. Weiss, *Quantum Dissipative Systems*, 4th ed. (World Scientific, Singapore, 2012).
- [2] H.-P. Breuer and F. Petruccione, *The Theory of Open Quantum Systems* (Oxford University Press, New York, 2002).
- [3] H.-P. Breuer, E. M. Laine, J. Piilo, and B. Vacchini, *Rev. Mod. Phys.* **88**, 021002 (2016).
- [4] A. Rivas, S. F. Huelga, and M. B. Plenio, *Rep. Prog. Phys.* **77**, 094001 (2014).
- [5] I. de Vega and D. Alonso, *Rev. Mod. Phys.* **89**, 015001 (2017).
- [6] K. Krauss, *States, Effects and Operations: Fundamental Notions of Quantum Theory* (Springer, Berlin, 1983).
- [7] K. Krauss, *Quantum Dynamical Semigroups and Applications* (Springer, Berlin, 1983).
- [8] V. May and O. Kühn, *Charge and Energy Transfer in Molecular Systems*, (Wiley-VCH, Berlin, 2011).
- [9] S. J. Glaser, U. Boscain, T. Calarco, C. P. Koch, W. Köckenberger, R. Kosloff, I. Kuprov, B. Luy, S. Schirmer, T. Schulte-Herbrüggen, D. Sugny, and F. K. Wilhelm, *Eur. Phys. J. D* **69**, 279 (2015).
- [10] C. P. Koch, *J. Phys.: Condens. Matter* **28**, 213001 (2016).
- [11] A. W. Chin, J. Prior, R. Rosenbach, F. Caycedo-Soler, S. F. Huelga, and M. B. Plenio, *Nat. Phys.* **9**, 113 (2013).
- [12] S. Gélinas, A. Rao, A. Kumar, S. L. Smith, A. W. Chin, J. Clark, T. S. van der Poll, G. C. Bazan, and R. H. Friend, *Science* **343**, 512 (2014).
- [13] G. D. Scholes, G. R. Fleming, A. Olaya-Castro, and R. van Grondelle, *Nat. Chem.* **3**, 763 (2011).
- [14] W. Pötz, *Appl. Phys. Lett.* **89**, 254102 (2006).
- [15] M. Wenin and W. Pötz, *Appl. Phys. Lett.* **92**, 103509 (2008).
- [16] M. Grace, C. Brif, H. Rabitz, I. A. Walmsley, R. I. Kosut, and D. A. Lidar, *J. Phys. B: At. Mol. Opt. Phys.* **40**, S103 (2007).
- [17] W. Cui, Z. R. Xi, and Y. Pan, *Phys. Rev. A* **77**, 032117 (2008).
- [18] J.-S. Tai, K.-T. Lin, and H.-S. E. Goan, *Phys. Rev. A* **89**, 062310 (2014).
- [19] R. Schmidt, A. Negretti, J. Ankerhold, T. Calarco, and J. T. Stockburger, *Phys. Rev. Lett.* **107**, 130404 (2011).
- [20] P. Reberntrost, I. Serban, T. Schulte-Herbrüggen, and F. K. Wilhelm, *Phys. Rev. Lett.* **102**, 090401 (2009).
- [21] D. M. Reich, N. Katz, and C. P. Koch, *Sci. Rep.* **5**, 12430 (2015).
- [22] P. M. Poggi, M. C. Lombardo, and D. A. Wisniacki, *Europhys. Lett.* **118**, 20005 (2017).
- [23] R. Puthumpally-Joseph, O. Atabek, E. Mangaud, M. Desouter-Lecomte, and D. Sugny, *Mol. Phys.* **115**, 1944 (2017).
- [24] E. Mangaud, R. Puthumpally-Joseph, D. Sugny, C. Meier, O. Atabek, and M. Desouter-Lecomte, *New J. Phys.* (to be published), doi:10.1088/1367-2630/aab651.
- [25] C. Meier and D. J. Tannor, *J. Chem. Phys.* **111**, 3365 (1999).
- [26] Y. Ohtsuki, *J. Chem. Phys.* **119**, 661 (2003).
- [27] R. Xu, Y. Yan, Y. Ohtsuki, Y. Fujimura, and H. Rabitz, *J. Chem. Phys.* **120**, 6600 (2004).
- [28] R. Sampaio, S. Suomela, R. Schmidt, and T. Ala-Nissila, *Phys. Rev. A* **95**, 022120 (2017).
- [29] R. Schmidt, M. F. Carusela, J. P. Pekola, S. Suomela, and J. Ankerhold, *Phys. Rev. B* **91**, 224303 (2015).
- [30] C. Addis, E.-M. Laine, C. Gneiting, and S. Maniscalco, *Phys. Rev. A* **94**, 052117 (2016).
- [31] D. Basilewitsch, R. Schmidt, D. Sugny, S. Maniscalco, and C. P. Koch, *New J. Phys.* **19**, 113042 (2017).
- [32] A. J. Leggett, S. Chakravarty, A. T. Dorsey, M. P. A. Fisher, A. Garg, and W. Zwerger, *Rev. Mod. Phys.* **59**, 1 (1987).
- [33] H. Tamura, I. Burghardt, and M. Tsukada, *J. Phys. Chem. C* **115**, 10205 (2011).
- [34] H. Tamura, R. Martinazzo, M. Ruckebauer, and I. Burghardt, *J. Chem. Phys.* **137**, 22A540 (2012).
- [35] E. Mangaud, C. Meier, and M. Desouter-Lecomte, *Chem. Phys.* **494**, 90 (2017).
- [36] Y. Tanimura and R. Kubo, *J. Phys. Soc. Jpn.* **58**, 101 (1989).
- [37] A. Ishizaki and Y. Tanimura, *J. Phys. Soc. Jpn.* **74**, 3131 (2005).
- [38] Y. Tanimura, *J. Phys. Soc. Jpn.* **75**, 082001 (2006).
- [39] S. Lorenzo, F. Plastina, and M. Paternostro, *Phys. Rev. A* **88**, 020102 (2013).
- [40] L. A. Pachón and P. Brumer, *J. Chem. Phys.* **139**, 164123 (2013).
- [41] J. Xu, R. X. Xu, and Y. J. Yan, *New J. Phys.* **11**, 105037 (2009).
- [42] H. D. Zhang and Y. J. Yan, *J. Chem. Phys.* **143**, 214112 (2015).
- [43] See Supplemental Material at <http://link.aps.org/supplemental/10.1103/PhysRevA.97.033411> to illustrate the time evolution of the volume of accessible states.
- [44] H. Stapelfeldt and T. Seideman, *Rev. Mod. Phys.* **75**, 543 (2003).
- [45] A. Chenel, E. Mangaud, I. Burghardt, C. Meier, and M. Desouter-Lecomte, *J. Chem. Phys.* **140**, 044104 (2014).

- [46] A. Pomyalov, C. Meier, and D. J. Tannor, *Chem. Phys.* **370**, 98 (2010).
- [47] L. Zhu, H. Liu, W. Xie, and Q. Shi, *J. Chem. Phys.* **137**, 194106 (2012).
- [48] U. Fano, *Phys. Rev.* **124**, 1866 (1961).
- [49] D. Finkelstein-Shapiro, I. Urdaneta, M. Calatayud, O. Atabek, V. Mujica, and A. Keller, *Phys. Rev. Lett.* **115**, 113006 (2015).
- [50] G. Clos and H.-P. Breuer, *Phys. Rev. A* **86**, 012115 (2012).
- [51] H.-P. Breuer, E. M. Laine, and J. Piilo, *Phys. Rev. Lett.* **103**, 210401 (2009).
- [52] S. Lorenzo, F. Plastina, and M. Paternostro, *Phys. Rev. A* **84**, 032124 (2011).
- [53] M. J. W. Hall, J. D. Cresser, L. Li, and E. Anderson, *Phys. Rev. A* **89**, 042120 (2014).
- [54] E. Anderson, J. D. Cresser, and M. J. W. Hall, *J. Mod. Opt.* **54**, 1695 (2007).
- [55] S. Haseli, S. Salimi, and A. S. Khorashad, *Quantum Inf. Process.* **14**, 3581 (2015).
- [56] D. Sugny, S. Vranckx, M. Ndong, N. Vaeck, O. Atabek, and M. Desouter-Lecomte, *Phys. Rev. A* **90**, 053404 (2014).